ACS Medicinal Chemistry Letters

pubs.acs.org/acsmedchemlett

Letter

Discovery of Thieno[3,2-*b*]pyridine-5-carboxamide and 2,3-Difluorobenzamide Negative Allosteric Modulators of Metabotropic Glutamate Receptor Subtype 5

Katherine E. Crocker,*,▽ Scott H. Henderson,▽ Rory A. Capstick, David L. Whomble, Aaron M. Bender, Andrew S. Felts, Changho Han, Julie L. Engers, Natasha B. Billard, Mallory A. Maurer, Hyekyung P. Cho, Alice L. Rodriguez, Colleen M. Niswender, Jordan O'Neill, Katherine J. Watson, Sichen Chang, Anna L. Blobaum, Olivier Boutaud, Weimin Peng, Jerri M. Rook, P. Jeffrey Conn, Craig W. Lindsley, and Kayla J. Temple*

Cite This: *ACS Med. Chem. Lett.* 2025, 16, 865−874

Read Online

ABSTRACT: This Letter describes the discovery of novel $mGlu_5$ NAMs **VU6031545** and **VU6024945**. Starting from previously reported picolinamide compounds, a structure−activity relationship study of various core isosteres was conducted, leading to the identification of thieno[3,2-*b*]pyridine-5-carboxamide and 2,3-difluorobenzamide as competent core replacements. These compounds are highly potent as well as brain penetrant with an IVIVC agreement and improved oral bioavailability in rats.

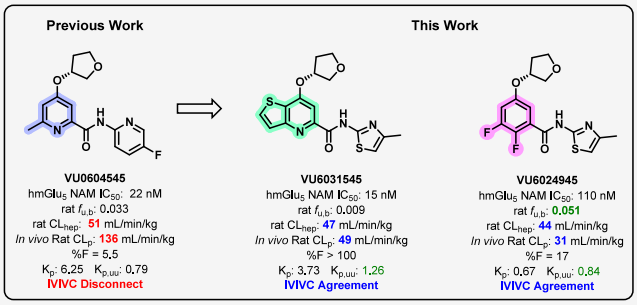

KEYWORDS: *Metabotropic Glutamate Receptor Subtype 5, $mGlu_5$, Negative Allosteric Modulator (NAM), Structure Activity Relationship (SAR), Isostere, Levodopa-Induced Dyskinesia, Pain*

L-Glutamate is the major excitatory neurotransmitter of the mammalian central nervous system (CNS) and modulates the activity of the metabotropic glutamate (mGlu) receptors. The eight mGlu receptor subtypes ($mGlu_{1-8}$) are divided into three groups (groups I, II, and III) based on structure/sequence homology, downstream signaling partners, and pharmacology. Group I metabotropic glutamate receptors (i.e., $mGlu_1$ and $mGlu_5$) are broadly expressed in the mammalian nervous system and are primarily found postsynaptically where they play a key role in modulating synaptic plasticity.[1] Predominately coupled via G_q, activation of $mGlu_5$ by glutamate regulates the function of phospholipase C, which, in turn, releases Ca^{2+} from intracellular stores.[2,3] All eight mGlu receptors have a seven transmembrane (7TM) α-helical domain that connects to a large "Venus fly trap (VFT)" domain. While glutamate binds to the orthosteric site located within the VFT domain, allosteric sites have been identified within the transmembrane domain.[4] Due to the highly conserved nature of the orthosteric binding site, successful design of selective orthosteric ligands has proven difficult. Therefore, research in the field has shifted focus toward allosteric modulation as an approach to improve selectivity when targeting specific mGlu subtypes. With over a decade of research, $mGlu_5$ NAMs are some of the most extensively studied and advanced within the realm of mGlu allosteric modulation.[5−7] As such, several $mGlu_5$ NAMs have been evaluated and demonstrated efficacy both preclinically and clinically, further establishing the utility of a selective $mGlu_5$ NAM in a multitude of potential therapeutic applications including levodopa-induced dyskinesia (LID) associated with Parkinson's disease,[8] fragile X syndrome,[9] autism spectrum disorder,[10] gastroesophageal reflux disease (GERD),[11] substance abuse disorder,[12] anxiety,[13] major depressive disorder,[14] obsessive-compulsive disorder (OCD),[15] Alzheimer's disease,[16] migraine,[17] and pain.[18]

Early $mGlu_5$ NAM tool compounds MPEP (**1**) and MTEP (**2**) share a biaryl/heterobiaryl acetylene motif as the key pharmacophore which was retained throughout subsequent medicinal chemistry campaigns (Figure 1, analogues **3**−**6**, highlighted in blue). It is well-documented that acetylenes are potentially reactive functional groups and can pose metabolic

Received: March 5, 2025
Revised: April 10, 2025
Accepted: April 16, 2025
Published: April 22, 2025

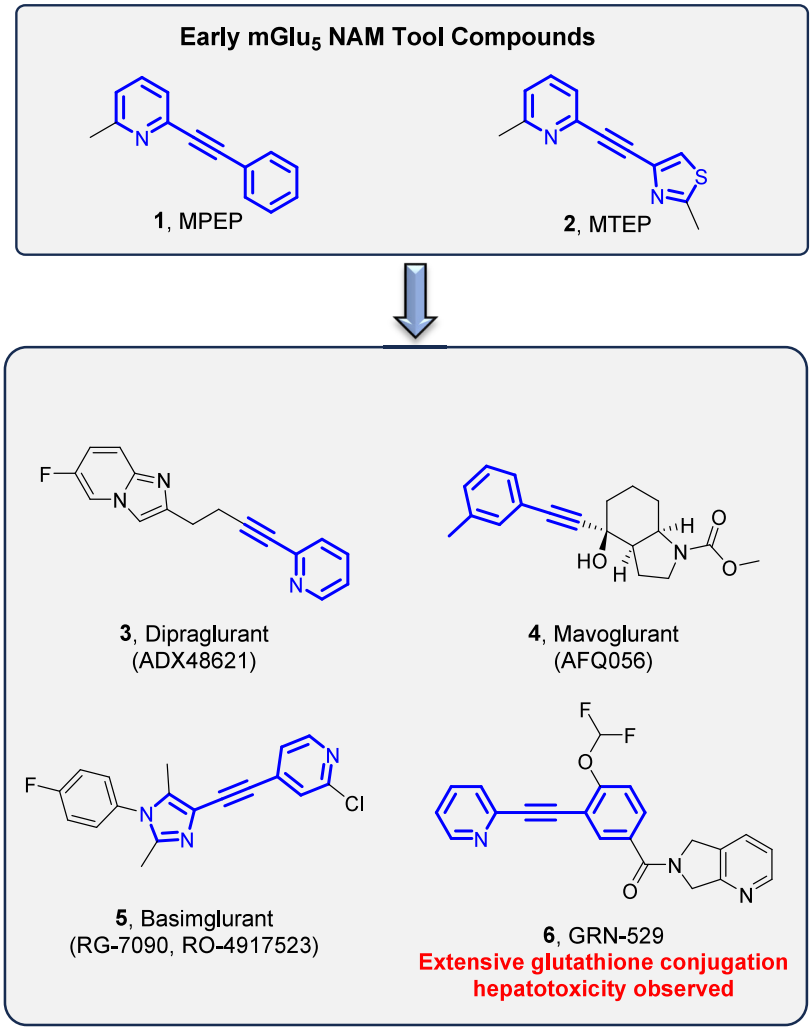

Figure 1. Selective $mGlu_5$ NAMs based on an aryl/heterobiaryl acetylene pharmacophore (highlighted in blue).

liabilities. For instance, the $mGlu_5$ NAM GRN-529 (**6**) demonstrated extensive glutathione conjugation to the alkyne which is believed to have resulted in biliary epithelial hyperplasia in nonhuman primates (NHPs) during an 8-week regulatory toxicology study.[19] Attempts to develop nonacetylene based NAMs resulted in the discovery of fenobam (**7**) and AZD9272 (**8**) which were both advanced into clinical trials (Figure 2). Unfortunately, the development of psychosis-like symptoms led to the termination of these trials. It is important to note that further studies attributed these side effects to off-target engagement of monoamine oxidase-B (MAO-B)-mediated mechanisms and not mechanisms facilitated by the $mGlu_5$ receptor.[20] At present, TMP-301 (**9**) is the only nonacetylene-based $mGlu_5$ NAM undergoing clinical trials (Phase I) for substance abuse disorders.[21] Interestingly, TMP-301 (**9**) and AZD9272 (**8**) are structurally very similar (highlighted in Figure 2); thus, TMP-301 may also suffer from off-target side effects (MAO-B). Currently, no $mGlu_5$ NAM has successfully progressed through clinical trials, highlighting the continued need for structurally diverse $mGlu_5$ NAMs.

A major focus of our group has been the development of small molecule $mGlu_5$ NAMs (Figure 3). Our work led to the identification of preclinical candidate **VU0424238** (**10**) (Figure 3).[22] In a 28-day toxicology study, a NHP species-

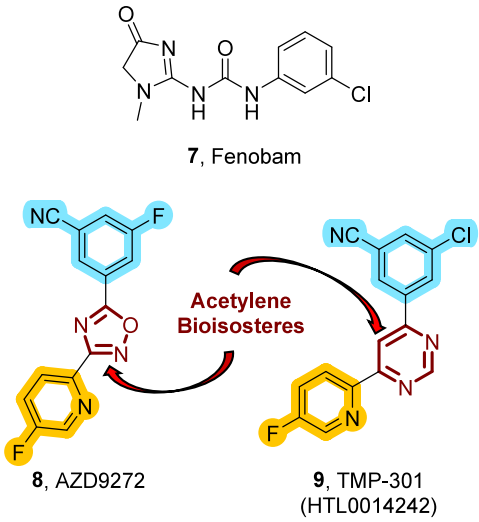

Figure 2. Nonacetylene, selective $mGlu_5$ NAMs.

specific aldehyde oxidase (AO) metabolite accumulated after 14 days, resulting in pronounced anemia (nonmechanism based); therefore, further development of **10** was halted. Detailed metabolic studies has shown that in NHPs, the pyrimidine headgroup is oxidized by AO, whereas, in rats, this

https://doi.org/10.1021/acsmedchemlett.5c00119
ACS Med. Chem. Lett. 2025, 16, 865−874

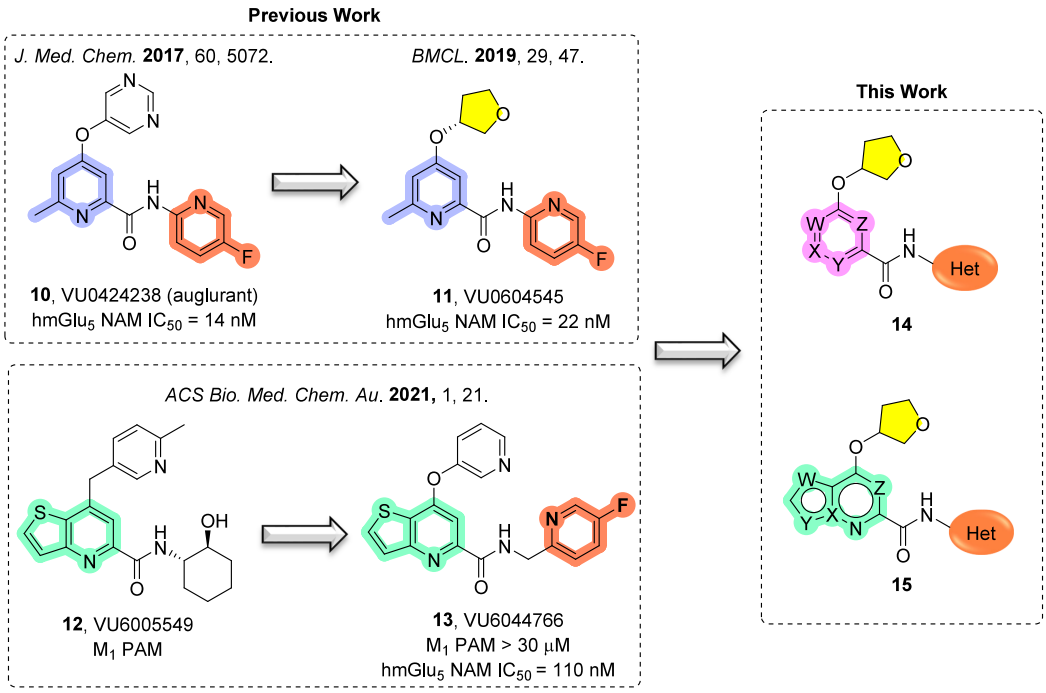

Figure 3. Previously published scaffold-hopping exercises that led to the discovery of $mGlu_5$ NAMs **11** and **13**. Further medicinal chemistry efforts led to novel and potent $mGlu_5$ NAMs **14** and **15**.

Scheme 1. Synthesis of $mGlu_5$ NAM Analogues 19a−19g and 22[a]

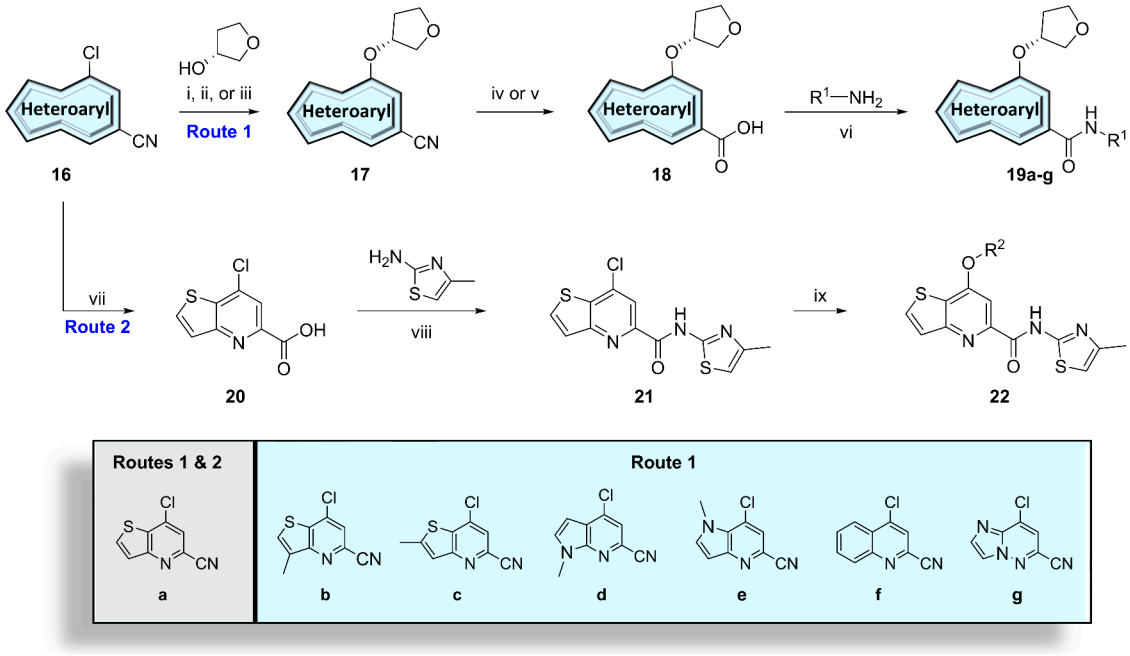

[a]Reagents and conditions: (i) KHMDS, DMF, 0 °C 1−18 h, 44%−92%; (ii) KHMDS, DMF, 0−60 °C, 48 h, 63%−91% (for **19d**); (iii) K_2CO_3, DMF, microwave irradiation at 150 °C, 20 min, 61% (for **19g**); (iv) 2*M* $NaOH_{(aq)}$ or 2*M* $LiOH_{(aq)}$, 1,4-dioxane or THF, 60−100 °C, 2−8 h, 51%−100%; (v) 2*M* $NaOH_{(aq)}$, 1,4-dioxane, microwave irradiation at 120 °C, 30 min, 99%; (vi) $POCl_3$, R^1NH_2, pyridine, 23 °C, 30 min, 15%−95%; (vii) $NaOH_{(aq)}$, 1,4-dioxane, 100 °C, 18 h, 99%; (viii) $POCl_3$, pyridine, 23 °C, 30 min, 74%; (ix) R^2OH, KO^tBu, DMSO, 65 °C, 19%−97%.

oxidation process is carried out by xanthine oxidase (XO).[23] Thus, these observed AO/XO metabolism differences between species may be linked to the observed NHP-specific toxicity.

To eliminate AO/XO metabolism, we have published a follow-up series of compounds wherein the pyrimidine headgroup is replaced with a sp^3-hybridized headgroup as in **VU0604545**, **11** (Figure 3, highlighted in yellow).[24] Although potent when screened on human $mGlu_5$ ($hmGlu_5$ IC_{50} = 22 nM), compound **11** suffered several setbacks including high predicted hepatic clearance in rat (CL_{hep} = 51 mL/min/kg), as well as poor oral bioavailability (%F = 5.5). When assessed *in vivo*, clearance was determined to be 136 mL/min/kg, indicating an *in vitro*−*in vivo* correlation (IVIVC) disconnect. Alternatively, we have reported on a series of 7-alkoxy-

https://doi.org/10.1021/acsmedchemlett.5c00119
ACS Med. Chem. Lett. 2025, 16, 865−874

thieno[3,2-*b*]pyridine-5-carboxamides derived from an unexpected mode shift of an M_1 PAM scaffold **12** to generate $mGlu_5$ NAM **13** (Figure 3).[25] Compound **13** showed promising $mGlu_5$ potency ($hmGlu_5$ IC_{50} = 110 nM), was centrally penetrant (K_p = 0.94) and fully displaced radioligand [^{3}H]methoxyPEPy (K_i = 0.16 μM). Having discovered thieno[3,2-*b*]pyridine (Figure 3, green) as a competent core replacement, we performed a scaffold-hopping exercise to incorporate novel cores into our previously established sp^3-hybridized headgroup series. This endeavor resulted in potent $mGlu_5$ NAMs with increased sp^3 character that lack the metabolically labile pyrimidine found in compound **10** (Figure 3, analogues **14** and **15**).

To begin, we first synthesized 7-(tetrahydrofuran-3-yl)-thieno[3,2-*b*]pyridine-5-carboxamides with varying amide moieties (Figure 3, orange) as shown in Scheme 1 (Route 1). Reaction of nitrile **16a** with (*R*)-tetrahydrofuran-3-ol and base afforded nitrile **17a**, which was subsequently hydrolyzed to intermediate carboxylic acid **18a** using sodium hydroxide. Conversion to the acid chloride using phosphorus oxychloride and *in-situ* trapping with various heterocyclic amines generated analogues **19a**, which were screened against human $mGlu_5$ to determine potency, with the results highlighted in Table 1. Gratifyingly, the replacement of the picolinamide core with thieno[3,2-*b*]pyridine in the context of the (*R*)-tetrahydrofuranyl ether and 5-fluoropyridyl amide led to a compound with similar potency as **11** (**19aB**: $hmGlu_5$ IC_{50} = 61 nM). Interestingly, moving the fluoro substituent from the 5-position to the 6-position of the pyridine amide led to a >17-fold reduction in potency (**19aC**: $hmGlu_5$ IC_{50} = 1.1 μM); however, substitution with a methyl group at the 6-position resulted in a 3-fold improvement in potency (**19aD**: $hmGlu_5$ IC_{50} = 22 nM). Exchanging the pyridine ring of **19aD** with a phenyl ring gave a 40-fold loss in activity (**19aE**: $hmGlu_5$ IC_{50} = 845 nM). Exchanging the pyridine ring with a pyrazine was even more detrimental to potency (**19aF**: $hmGlu_5$ IC_{50} > 10 μM). Replacement of the 5-methylpyridine with a 4-methylthiazole, a common isostere, provided an analog with similar potency (**19aA**: $hmGlu_5$ IC_{50} = 15 nM). Steric bulk on the thiazole amide was not well-tolerated (**19aH−19aJ**), nor was the removal of the methyl substituent (**19aK**). Incorporation of fluorine(s) onto the 4-methylthiazole ring resulted in a slight drop in potency (**19aL**: $hmGlu_5$ IC_{50} = 55 nM; **19aM**: $hmGlu_5$ IC_{50} = 320 nM). Similarly, the addition of an electron-withdrawing group also led to a loss of activity (**19aN:** $hmGlu_5$ IC_{50} = 559 nM). Moreover, alternative 5-membered heterocyclic amides were not tolerated (**19aP-R**). Taken together with our previous works, amide preference varied, depending upon the core scaffold employed with no obvious SAR trends identified.

Table 1. Structures and Activities for Analogs 19aA-aR[a]

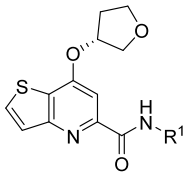

19a

Cmpd.	R[1]	pIC_{50} [%Glu_{min}] IC_{50} (nM)	Cmpd.	R[1]	pIC_{50} [%Glu_{min}] IC_{50} (nM)
19aA		7.84 2 15	**19aJ**		inactive
19aB		7.22 2 61	**19aK**		5.75 3 1830
19aC		5.98 6 1070	**19aL**		7.27 2 55
19aD		7.66 2 22	**19aM**		6.50 18 320
19aE		6.08 2 845	**19aN**		6.27 3 559
19aF		<5 44 >10,000	**19aO**		5.97 3 1110
19aG		<5 66 >10,000	**19aP**		<5 50 >10,000
19aH		5.62 6 2557	**19aQ**		<5 73 >10,000
19aI		inactive	**19aR**		inactive

[a]Calcium mobilization assays in human $mGlu_5$-HEK293A cells were performed in the presence of an EC_{80} fixed concentration of glutamate, n = 2 independent experiments in triplicate. The % Glu_{Min} is the measure of efficacy of the NAM to reduce an EC_{80} response of glutamate.

Next, we shifted our attention to the optimization of the headgroup (Figure 3, yellow) in the context of the 4-methylthiazole amide. To generate these analogues, as shown in Scheme 1 (Route 2), nitrile **16a** was first hydrolyzed to the corresponding carboxylic acid **20**. Following acid chloride formation with phosphorus oxychloride, *in-situ* coupling with 4-methylthiazol-2-amine gave rise to the key intermediate **21**. Finally, chloride **21** underwent nucleophilic aromatic substitution with various alcohols to generate compounds **22**, which were screened against human $mGlu_5$ with results reported in Table 2. These results highlight the importance of the ether-containing headgroup. When compared to the picolinamide series **11**, several similar SAR trends were noted. For instance, the (*R*)-tetrahydrofuranyl enantiomer (**19aA**: $hmGlu_5$ IC_{50} = 15 nM) is preferred to the (*S*)-enantiomer (**22a**: $hmGlu_5$ IC_{50} = 543 nM), with a 36-fold difference in potency. Additionally, steric bulk (**22b**) and ring expansion (**22c** and **22d**) were not tolerated and detrimental to potency. Another similarity was observed when ring contraction to the oxetane resulted in a moderately potent compound (**22e**: $hmGlu_5$ IC_{50} = 185 nM), a 12-fold loss in activity was observed when compared to **19aA**. Likewise, both the cyclobutanecarbonitrile (**22i**) and thietane (**22j**) analogues also gave an ∼7-fold loss in potency. Like the picolinamide series, homologation to the methylene tetrahydrofuranyl analogue led to an 18-fold loss in potency (**22f**: $hmGlu_5$ IC_{50} = 267 nM). Also, conversion from furanyl (**19aA**) to cyclopentyl resulted in a drastic loss of potency (**22h**: $hmGlu_5$ IC_{50} > 10 μM), emphasizing the importance of the heteroatom in the ether headgroup.

We next investigated other core replacements of the picolinamide of **11** (Figure 3, blue) while holding constant the (*R*)-tetrahydrofuranyl ether and both the methylthiazoleamide and 5-fluoropyridyl amide tails. Synthesis of these analogues followed a similar strategy from easily accessible starting materials, as shown in Schemes 1 and 2. First, various nitriles **16b−16g** underwent a series of reactions

https://doi.org/10.1021/acsmedchemlett.5c00119
ACS Med. Chem. Lett. 2025, 16, 865−874

Table 2. Structures and Activities for Analogues 22a−22j[a]

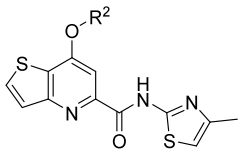

22

Cmpd.	R²	pIC50 [%Glumin] IC50 (nM)	Cmpd.	R²	pIC50 [%Glumin] IC50 (nM)
22a		6.30 2 543	**22f**		6.60 2 267
22b		inactive	**22g**		6.17 12 682
22c		6.46 2 367	**22h**		<5 20 >10,000
22d		<5 25 >10,000	**22i**		7.03 2 99
22e		6.76 2 185	**22j**		6.98 2 107

[a]Calcium mobilization assays in human $mGlu_5$-HEK293A cells were performed in the presence of an EC_{80} fixed concentration of glutamate, $n = 2$ independent experiments in triplicate. The % Glu_{Min} is the measure of efficacy of the NAM to reduce an EC_{80} response of glutamate.

as previously described for the thieno[3,2-*b*]pyridine core analogues to afford compounds **19b−19g** (Scheme 1, Route 1). The remaining analogues were synthesized through various ester intermediates that could be easily obtained and subsequently hydrolyzed before performing an amide formation. In the case of the pyridazine core, an S_NAr reaction between 3,5-dichloropyridazine (**23a**) and (*R*)-tetrahydrofuran-3-ol gave the chloride intermediate **24a** which was subsequently converted to ester intermediate **25a** via palladium-catalyzed carbonylation in ethanol (Scheme 2, Route 1). For aryl/heteroaryl alcohols, such as ethyl 5-hydroxynicotinate (**28b**) and ethyl 2,3-difluoro-5-hydroxybenzoate (**28c**), Mitsunobu reactions with (*S*)-tetrahydrofuran-3-ol afforded the alkyl ether intermediates **25b** and **25c** (Scheme 2, Route 2). Finally, chlorides **30e−30g** underwent an S_NAr reaction with (*R*)-tetrahydrofuran-3-ol to afford ester intermediates **25e−25g** (Scheme 2, Route 4). With intermediates **25a−25c** and **25e−25g** in hand, ester hydrolysis under basic conditions provided carboxylic acid intermediates **26** in quantitative yield. Alternatively, direct nucleophilic aromatic substitution reaction between commercial carboxylic acid **29d** with (*R*)-tetrahydrofuran-3-ol afforded carboxylic acid **26d** in quantitative yield (Scheme 2, Route 3). With the requisite acid intermediates in hand, reactions with phosphorus oxychloride and either 5-fluoropyridin-2-amine or 4-methylthiazol-2-amine in pyridine afforded compounds **27a−27g** in low to modest yields. Compounds **19b−19g** and **27a−27g** were screened against human $mGlu_5$ to determine potency with the results highlighted in Table 3.

We quickly noticed varying the pyridine regiochemistry of the picolinamide core resulted in a complete loss of potency (**27bA-B**). Other 6-membered nitrogen-containing heterocycles including pyridazine (**27aA-B**), pyrazine (**27dA-B**), and pyrimidine (**27eA-B**) were similarly unsuccessful. These results demonstrate the importance of the nitrogen position within the pyridine ring of the picolinamide core. Notably, the 1,2-difluorobenzyl core was a competent picolinamide replacement in the context of the 4-methylthiazole amide (**27cA**: $hmGlu_5$ IC_{50} = 110 nM); however, the 5-fluoropyridine amide was 14-fold less potent (**27cB**: $hmGlu_5$ IC_{50} = 1.6 μM). Throughout this exercise, this general trend was observed, indicating the importance of the amide tail substitution.

Postulating that the methyl substitution of the pyridine core of compounds **10** and **11** was important for maintaining potency, we returned our attention to bicyclic ring systems to mimic the methyl substitution with alternative 5,6- or 6,6-fused heteroaryl ring systems. While the quinoline core provided a modestly potent analogue in the context of the 4-methylthiazole amide (**19fA**: $hmGlu_5$ IC_{50} = 192 nM), the addition of a nitrogen atom to give a 1,7-naphthyridine core was detrimental to potency (**27gA**: $hmGlu_5$ IC_{50} = 2.1 μM). Similarly, addition of a second nitrogen to the thieno[3,2-*b*]pyridine ring of **19a** to generate the thieno[3,2-*d*]pyrimidine also resulted in a loss of potency (**27fA**: $hmGlu_5$ IC_{50} = 1.2 μM) as did substitutions on the thieno[3,2-*b*]pyridine ring (**19bA**: $hmGlu_5$ IC_{50} = 328 nM; **19cA**: $hmGlu_5$ IC_{50} = 357 nM). Other core replacements such as 1-methyl-1*H*-pyrrolo-[3,2-*b*]pyridine (**19e**) and imidazo[1,2-*b*]pyridazine (**19g**) proved to be ineffective. Conversely, the 1-methyl-1*H*-pyrrolo[2,3-*b*]pyridine core delivered a potent $mGlu_5$ NAM (**19dA**: $hmGlu_5$ IC_{50} = 93 nM).

To determine which compounds would be advanced into extensive *in vitro* and *in vivo* drug metabolism and pharmacokinetic (DMPK) characterization, we initially evaluated rat predicted hepatic clearance (CL_{hep}) and human plasma fraction unbound ($f_{u,plasma}$) of our most potent analogues ($hmGlu_5$ $IC_{50} \leq 110$ nM) as a method to quickly triage compounds (results highlighted in Table 4). Many of the

https://doi.org/10.1021/acsmedchemlett.5c00119
ACS Med. Chem. Lett. 2025, 16, 865−874

Scheme 2. Synthesis of mGlu$_5$ NAM Analogues 27a−27g[a]

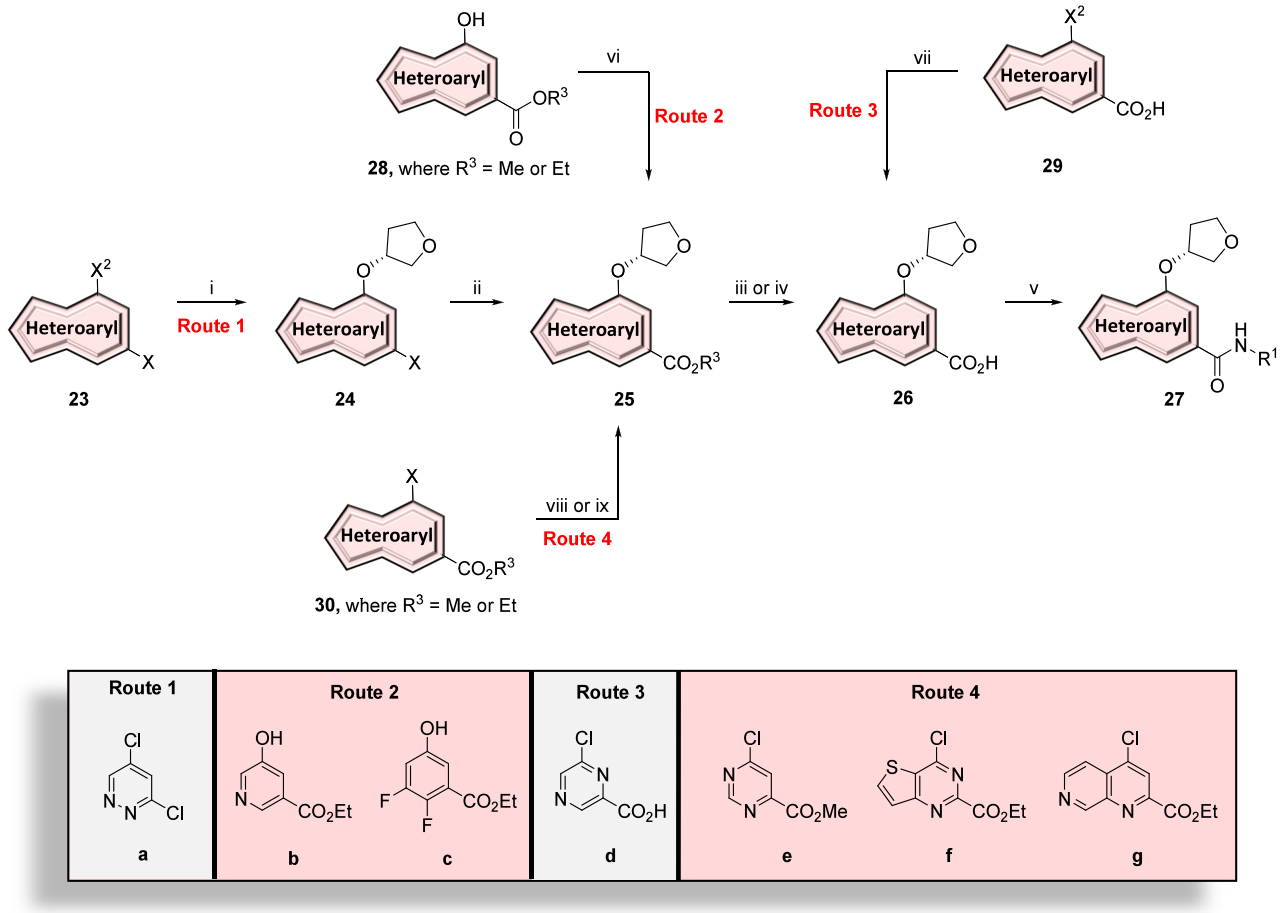

[a]Reagents and conditions: (i) (*R*)-tetrahydrofuran-3-ol, NaH, NMP, 0−23 °C, 1 h, 36%; (ii) Pd(dppf)Cl_2•DCM, NaOAc, EtOH/DMF, $CO_{(g)}$, 70 °C, 3 h, 90%; (iii) 2*M* $NaOH_{(aq)}$ or 2*M* $LiOH_{(aq)}$, THF, 1−2 h, 85%−99%; (iv) 2*M* $LiOH_{(aq)}$, THF, 60 °C, 8 h, 85% (for **30f**); (v) $POCl_3$, R^1NH_2, pyridine, 23 °C, 30 min, 2%−47%; (vi) (*S*)-tetrahydrofuran-3-ol, DIAD, PPh_3, THF, 23 °C, 1 h, 62%−74%; (vii) (*R*)-tetrahydrofuran-3-ol, KHMDS, THF, microwave irradiated at 150 °C, 15 min, 99%; (viii) (*R*)-tetrahydrofuran-3-ol, KO^{t}Bu, DMF, 80 °C, 30 min, 99% (for **30e**); (ix) (*R*)-tetrahydrofuran-3-ol, KHMDS, DMF, 0 °C, 30 min, 58%−72% (for **30f**−**30g**).

analogues displayed high rat predicted CL_{hep} based on *in vitro* microsomal data (>47 mL/min/kg); however, analogues **19aA**, **19aL**, and **27cA** were predicted to have moderate rat CL_{hep} (44−47 mL/min/kg), compared to the predecessor compound **VU0604545** (**11**) (CL_{hep} = 51 mL/min/kg). Of these three compounds, **19aA** ($f_{u,plasma}$ = 0.020) and **27cA** ($f_{u,plasma}$ = 0.069) were determined to have the most attractive human plasma fraction unbound. Based on these data, **19aA** (**VU6031545**) and **27cA** (**VU6024945**) were selected to advance into a battery of *in vitro* and *in vivo* DMPK assays and our standard rat plasma:brain level (PBL) cassette studies (Table 5).

Regarding physicochemical properties, both compounds possessed molecular weights less than 365 Da with attractive *x* Log *P* values (<4) for CNS penetration. Although both compounds were predicted to have moderate clearance in rats, both were predicted to have high clearance in human (CL_{hep} > 15 mL/min/kg). While both compounds exhibited moderate plasma free faction in rat, **VU6024945** demonstrated a more desirable fraction unbound in rat brain homogenates ($f_{u,brain}$ = 0.051) versus **VU6031545** ($f_{u,brain}$ = 0.009). Although **VU6024945** displayed sufficient CNS distribution of unbound drug (rat brain:plasma K_p = 0.67; $K_{p,uu}$ = 0.84), **VU6031545** proved to have higher CNS penetration (rat brain:plasma K_p = 3.73; $K_{p,uu}$ = 1.29). When cytochrome P450 (CYP450) inhibition was evaluated, both analogues displayed a CYP1A2 IC_{50} ≤ 1.3 μM with no appreciable inhibition observed for the other isoforms tested (CYP 2C9, 2D6, 3A4 IC_{50} > 30 μM).

Due to the previous IVIVC disconnect observed for the **VU0604545** (**11**) series, we accessed both compounds in *in-vivo* IV/PO PK experiments. Gratifyingly, the predicted rat clearance of both **VU6031545** (CL_{hep} = 47.0 mL/min/kg) and **VU6024945** (CL_{hep} = 43.7 mL/min/kg) were in good agreement with the *in-vivo* clearances (CL_p = 49.3 mL/min/kg and CL_p = 31.3 mL/min/kg, respectively). **VU6031545** displayed a high volume of distribution (V_{ss} = 6.67 L/kg) with an elimination half-life of 3.42 h and an oral bioavailability >100%. **VU6024945** demonstrated a moderate volume of distribution (V_{ss} = 2.89 L/kg) with an elimination half-life of 1.78 h and a lower oral bioavailability (%F = 17). Both compounds represent an improvement over the previous series (**11**), which showed an IVIVC disconnect, a short elimination half-life ($t_{1/2}$ = 46 min), and poor oral bioavailability (%F = 5.5). Moreover, when compared to the structurally similar predecessor analogue **VU0409106** (CYP1A2 IC_{50} < 100 nM,

https://doi.org/10.1021/acsmedchemlett.5c00119
ACS Med. Chem. Lett. 2025, 16, 865−874

Table 3. Structures and Activities for Analogues 19b−19f and 27a−27g[a]

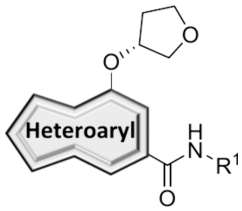

Cmpd.	Core Modification	R1 A: pIC50 [%Glumin] IC50 (nM)	R1 B: pIC50 [%Glumin] IC50 (nM)
19b	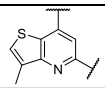	6.24 2 628	inactive
19c	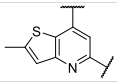	6.45 2 357	inactive
19d	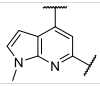	7.04 2 93	5.98 12 1060
19e	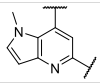	<5 10 >10,000	<5 46 >10,000
19f	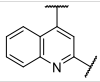	6.74 6 192	5.59 15 2650
19g		>5 52 >10,000	inactive
27a		inactive	inactive
27b		inactive	inactive
27c		6.99 2 110	5.88 3 1570
27d		inactive	inactive
27e		inactive	inactive
27f	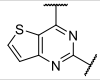	5.95 5 1170	5.18 9 7200
27g	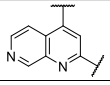	5.69 2 2050	5.76 3 1780

[a]Calcium mobilization assays in human $mGlu_5$-HEK293A cells were performed in the presence of an EC_{80} fixed concentration of glutamate, $n = 2$ independent experiments in triplicate. The % Glu_{Min} is the measure of efficacy of the NAM to reduce an EC_{80} response of glutamate.

%F < 5%), an analogue of **11** bearing a fluorophenyl core and methyl thiazole amide tail, incorporation of a sp^3-hybridized headgroup to provide **VU6024945** afforded improving drug-like properties (CYP1A2 IC_{50} = 1.3 μM, %F = 17%).[22]

Table 4. *In Vitro* Predicted Rat Hepatic Clearance (CL_{hep}) and Human Plasma Fraction Unbound ($f_{u,plasma}$) of the Most Potent $mGlu_5$ NAMs

compound	IC_{50} (nM)	rat CL_{hep} (mL/min/kg)	human $f_{u,plasma}$
19aA	15	47.0	0.020
19aB	61	55.1	0.008
19aD	22	57.5	0.005
19aL	55	41.8	0.016
19dA	93	52.3	0.006
22i	99	48.2	0.005
22j	107	68.4	0.001
27cA	110	43.7	0.069

Table 5. *In Vitro* and *In Vivo* DMPK Data for Analogues 19aA and 27cA

property	19aA, VU6031545	27cA, VU6024945
MW	361.43	340.34
x log P	3.23	3.23
TPSA	73.3	60.4
***In Vitro* PK Parameters**		
CL_{int} (mL/min/kg), rat	143	116
CL_{hep} (mL/min/kg), rat	47.0	43.7
CL_{int} (mL/min/kg), human	140	241
CL_{hep} (mL/min/kg), human	18.3	19.3
rat $f_{u,plasma}$[a]	0.027	0.040
human $f_{u,plasma}$[a]	0.020	0.069
Rat $f_{u,brain}$[a]	0.009	0.051
***In Vivo* PK Parameters[b]**		
CL_p (mL/min/kg)	49.3	31.3
Elim. $t_{1/2}$ (h)	3.42	1.78
MRT (h)	2.45	1.44
V_{ss} (L/kg)	6.67	2.89
%F[c]	>100	16.6
Brain Distribution (0.25 h) (SD Rat; 0.2 mg/kg IV)		
$K_{p\ brain:plasma}$[c]	3.73	0.67
$K_{p,uu\ brain:plasma}$[d]	1.29	0.84
CYP_{450} IC_{50} (μM)		
1A2	1.2	1.3
2C9	>30	>30
2D6	>30	>30
3A4	>30	>30

[a]f_u = fraction unbound; equilibrium dialysis assay; brain = rat brain homogenates. [b]Male Sprague−Dawley rats (n = 2); IV PK: 1 mg/kg, vehicle = 10% ethanol, 40% PEG400, 50% saline; PO PK: 10 mg/kg, vehicle = 10% Tween80 in water. [c]K_p = total brain-to-plasma partition ratio. [d]$K_{p,uu}$ = unbound brain-to-plasma partition ratio [(brain f_u × total brain)/(plasma f_u × total plasma)].

In conclusion, novel $mGlu_5$ NAMs were identified utilizing a scaffold hopping approach. Our new generation of $mGlu_5$ NAMs lack the classical aryl/heterobiaryl acetylene chemotype which has been linked to poor PK and hepatotoxicity. Utilizing thieno[3,2-*b*]pyridine-5-carboxamide as a core replacement for 6-methylpicolinomide of **VU0604545** (**11**), we were able to identify several potent $mGlu_5$ NAMs ($hmGlu_5$ IC_{50} < 80 nM). A follow-up exercise explored alternate cores and resulted in the discovery of additional highly potent $mGlu_5$ NAMs ($hmGlu_5$ IC_{50} ≤ 110 nM). Although many of these potent analogues displayed high predicted rat CL_{hep} and/or high plasma protein binding in human, two compounds (**19aA** and **27cA**) displayed moderate predicted clearance and moderate plasma fraction unbound in human. Both compounds were

https://doi.org/10.1021/acsmedchemlett.5c00119
ACS Med. Chem. Lett. 2025, 16, 865−874

advanced into further DMPK profiling. **VU6031545** (**19aA**) proved to be highly CNS penetrant (K_p = 3.73) with a high distribution of unbound drug ($K_{p,uu}$ = 1.29) which further improved upon predecessor compound **VU0604545** (**11**) (rat brain:plasma $K_{p,uu}$ = 0.79). Additionally, both **VU6031545** (**19aA**) and **VU6024945** (**27cA**) showed improvement in elimination half-life and oral bioavailability when compared to predecessor **VU0604545** (**11**). Unlike the previous series, these compounds showed good IVIVC. Unfortunately, both compounds were predicted to have high clearance in human (CL_{hep} > 15 mL/min/kg) and inhibited CYP1A2 ($IC_{50} \leq 1.3$ μM) and further progression was halted. While our current endeavor did not generate $mGlu_5$ NAMs with suitable DMPK profiles to warrant further development, it did provide invaluable SAR insights for future scaffold designs. Further refinements are underway and will be reported in due course.

■ ASSOCIATED CONTENT

Supporting Information

The Supporting Information is available free of charge at https://pubs.acs.org/doi/10.1021/acsmedchemlett.5c00119.

General methods for the synthesis and characterization of key compounds and experimental details for calcium mobilization assays, *in vitro* and *in vivo* DMPK protocols (PDF)

■ AUTHOR INFORMATION

Corresponding Authors

Kayla J. Temple − *Warren Center for Neuroscience Drug Discovery, Vanderbilt University, Nashville, Tennessee 37232, United States; Department of Pharmacology, Vanderbilt University School of Medicine, Nashville, Tennessee 37232, United States;* orcid.org/0000-0001-5290-574X; Phone: 615-343-2725; Email: kayla.temple@vanderbilt.edu

Katherine E. Crocker − *Warren Center for Neuroscience Drug Discovery, Vanderbilt University, Nashville, Tennessee 37232, United States; Department of Pharmacology, Vanderbilt University School of Medicine, Nashville, Tennessee 37232, United States*; Email: katherine.crocker@vanderbilt.edu

Authors

Scott H. Henderson − *Warren Center for Neuroscience Drug Discovery, Vanderbilt University, Nashville, Tennessee 37232, United States; Department of Pharmacology, Vanderbilt University School of Medicine, Nashville, Tennessee 37232, United States;* orcid.org/0000-0002-9504-5943

Rory A. Capstick − *Warren Center for Neuroscience Drug Discovery, Vanderbilt University, Nashville, Tennessee 37232, United States; Department of Pharmacology, Vanderbilt University School of Medicine, Nashville, Tennessee 37232, United States*

David L. Whomble − *Warren Center for Neuroscience Drug Discovery, Vanderbilt University, Nashville, Tennessee 37232, United States; Department of Pharmacology, Vanderbilt University School of Medicine, Nashville, Tennessee 37232, United States*

Aaron M. Bender − *Warren Center for Neuroscience Drug Discovery, Vanderbilt University, Nashville, Tennessee 37232, United States; Department of Pharmacology, Vanderbilt University School of Medicine, Nashville, Tennessee 37232, United States*

Andrew S. Felts − *Warren Center for Neuroscience Drug Discovery, Vanderbilt University, Nashville, Tennessee 37232, United States; Department of Pharmacology, Vanderbilt University School of Medicine, Nashville, Tennessee 37232, United States*

Changho Han − *Warren Center for Neuroscience Drug Discovery, Vanderbilt University, Nashville, Tennessee 37232, United States; Department of Pharmacology, Vanderbilt University School of Medicine, Nashville, Tennessee 37232, United States;* orcid.org/0000-0002-0832-7070

Julie L. Engers − *Warren Center for Neuroscience Drug Discovery, Vanderbilt University, Nashville, Tennessee 37232, United States; Department of Pharmacology, Vanderbilt University School of Medicine, Nashville, Tennessee 37232, United States;* orcid.org/0009-0004-3654-5464

Natasha B. Billard − *Warren Center for Neuroscience Drug Discovery, Vanderbilt University, Nashville, Tennessee 37232, United States; Department of Pharmacology, Vanderbilt University School of Medicine, Nashville, Tennessee 37232, United States*

Mallory A. Maurer − *Warren Center for Neuroscience Drug Discovery, Vanderbilt University, Nashville, Tennessee 37232, United States; Department of Pharmacology, Vanderbilt University School of Medicine, Nashville, Tennessee 37232, United States*

Hyekyung P. Cho − *Warren Center for Neuroscience Drug Discovery, Vanderbilt University, Nashville, Tennessee 37232, United States; Department of Pharmacology, Vanderbilt University School of Medicine, Nashville, Tennessee 37232, United States*

Alice L. Rodriguez − *Warren Center for Neuroscience Drug Discovery, Vanderbilt University, Nashville, Tennessee 37232, United States; Department of Pharmacology, Vanderbilt University School of Medicine, Nashville, Tennessee 37232, United States;* orcid.org/0000-0002-5244-5103

Colleen M. Niswender − *Warren Center for Neuroscience Drug Discovery, Vanderbilt University, Nashville, Tennessee 37232, United States; Department of Pharmacology, Vanderbilt University School of Medicine, Nashville, Tennessee 37232, United States; Department of Biochemistry, Vanderbilt University, Nashville, Tennessee 37232, United States; Vanderbilt Kennedy Center and Vanderbilt Brain Institute, Vanderbilt University School of Medicine, Nashville, Tennessee 37232, United States*

Jordan O'Neill − *Warren Center for Neuroscience Drug Discovery, Vanderbilt University, Nashville, Tennessee 37232, United States; Department of Pharmacology, Vanderbilt University School of Medicine, Nashville, Tennessee 37232, United States*

Katherine J. Watson − *Warren Center for Neuroscience Drug Discovery, Vanderbilt University, Nashville, Tennessee 37232, United States; Department of Pharmacology, Vanderbilt University School of Medicine, Nashville, Tennessee 37232, United States*

Sichen Chang − *Warren Center for Neuroscience Drug Discovery, Vanderbilt University, Nashville, Tennessee 37232, United States; Department of Pharmacology, Vanderbilt University School of Medicine, Nashville, Tennessee 37232, United States*

Anna L. Blobaum − *Warren Center for Neuroscience Drug Discovery, Vanderbilt University, Nashville, Tennessee 37232, United States; Department of Pharmacology, Vanderbilt*

University School of Medicine, Nashville, Tennessee 37232, United States

Olivier Boutaud − *Warren Center for Neuroscience Drug Discovery, Vanderbilt University, Nashville, Tennessee 37232, United States; Department of Pharmacology, Vanderbilt University School of Medicine, Nashville, Tennessee 37232, United States*

Weimin Peng − *Department of Pharmacology, Vanderbilt University School of Medicine, Nashville, Tennessee 37232, United States*

Jerri M. Rook − *Department of Pharmacology, Vanderbilt University School of Medicine, Nashville, Tennessee 37232, United States*

P. Jeffrey Conn − *Warren Center for Neuroscience Drug Discovery, Vanderbilt University, Nashville, Tennessee 37232, United States; Department of Pharmacology, Vanderbilt University School of Medicine, Nashville, Tennessee 37232, United States; Vanderbilt Brain Institute, Vanderbilt University School of Medicine, Nashville, Tennessee 37232, United States*

Craig W. Lindsley − *Warren Center for Neuroscience Drug Discovery, Vanderbilt University, Nashville, Tennessee 37232, United States; Department of Pharmacology, Vanderbilt University School of Medicine, Nashville, Tennessee 37232, United States; Department of Chemistry and Department of Biochemistry, Vanderbilt University, Nashville, Tennessee 37232, United States;* orcid.org/0000-0003-0168-1445

Complete contact information is available at:
https://pubs.acs.org/10.1021/acsmedchemlett.5c00119

Author Contributions

[∇]Authors K. E. Crocker and S. H. Henderson contributed equally to this work. S.H.H., R.A.C., D.L.W., A.M.B, A.S.F., C.H., J.L.E., and K.E.C. performed synthetic chemistry and provided chemical characterization. N.B.B., M.A.M., H.P.C., A.L.R., and C.M.N. performed and analyzed molecular pharmacology. W.P. and J.M.R. performed *in vivo* PK experiments. S.C., J.O., K.J.W., A.L.B., and O.B. performed and analyzed DMPK experiments. P.J.C, C.M.N., J.M.R, A.S.F., and C.W.L. oversaw experimental design, and K.E.C. and K.J.T. wrote the manuscript with input from all authors.

Notes

The authors declare the following competing financial interest(s): The authors hold IP on mGlu5 NAMs.

■ ACKNOWLEDGMENTS

We thank the NIH for funding via the Molecular Libraries Probe Center Network (No. U54MH084659, to C.W.L.), Vanderbilt NCDDG grants (Nos. U01MH087965 and U19MH097056, to P.J.C.), and the HEAL Initiative (No. 1UG3NS116218-01, to J.M.R and C.W.L). We also thank William K. Warren, Jr. and the William K. Warren Foundation who funded the William K. Warren, Jr. Chair in Medicine (to C.W.L.).

■ REFERENCES

(1) Bikbaev, A.; Manahan-Vaughan, D. Metabotropic glutamate receptor, $mGlu_5$, regulates hippocampal synaptic plasticity and is required for tetanisation-triggered changes in theta and gamma oscillations. *Neuropharmacology.* **2017**, *115*, 20−29.

(2) Golubeva, A. V.; Moloney, R. D.; O'Connor, R. M.; Dinan, T. G.; Cryan, J. F. Metabotropic glutamate receptors in central nervous system disease. *Curr. Drug Targets* **2016**, *17*, 538−616.

(3) Conn, P. J.; Pin, J. P. Pharmacology and functions of metabotropic glutamate receptors. *Annu. Rev. Pharmacol. Toxicol.* **1997**, *37*, 205−237.

(4) Melancon, B. J.; Hopkins, C. R.; Wood, M. R.; Emmitte, K. A.; Niswender, C. M.; Christopoulos, A.; Conn, P. J.; Lindsley, C. W. Allosteric modulation of seven transmembrane spanning receptors: theory, practice, and opportunities for central nervous system drug discovery. *J. Med. Chem.* **2012**, *55*, 1445−64.

(5) Emmitte, K. A. $mGlu_5$ negative allosteric modulators: a patent review (2013−2016). *Expert Opin. Ther. Pat.* **2017**, *27*, 691.

(6) Emmitte, K. A. Recent Advances in the Design and Development of Novel Negative Allosteric Modulators of $mGlu_5$. *ACS Chem. Neurosci.* **2011**, *2*, 411−432.

(7) Hao, J.; Xiong, H. SAR Studies on $mGlu_5$ Receptor Positive Allosteric Modulators (2003−2013). *Curr. Top. Med. Chem.* **2014**, *14*, 1789−1841.

(8) Rascol, O.; Fox, S.; Gasparini, F.; Kenney, C.; Di Paolo, T.; Gomez-Mancilla, B. Use of metabotropic glutamate 5-receptor antagonists for treatment of levodopa-induced dyskinesias. *Parkinsonism Relat. Disord.* **2014**, *20*, 947−956.

(9) Pop, A. S.; Gomez-Mancilla, B.; Neri, G.; Willemsen, R.; Gasparini, F. Fragile X syndrome: a preclinical review on metabotropic glutamate receptor 5 ($mGluR_5$) antagonists and drug development. *Psychopharmacology* **2014**, *231*, 1217.

(10) Silverman, J. L.; Smith, D. G.; Rizzo, S. J.; Karras, M. N.; Turner, S. M.; Tolu, S. S.; Bryce, D. K.; Smith, D. L.; Fonseca, K.; Ring, R. H.; Crawley, J. N. Negative Allosteric Modulation of the $mGluR_5$ Receptor Reduces Repetitive Behaviors and Rescues Social Deficits in Mouse Models of Autism. *Sci. Transl. Med.* **2012**, *4*, 131ra51.

(11) Zerbib, F.; Bruley des Varannes, S.; Roman, S.; Tutuian, R.; Galmiche, J. P.; Mion, F.; Tack, J.; Malfertheiner, P.; Keywood, C. Randomized clinical trial: effects of monotherapy with ADX10059, a $mGluR_5$ inhibitor, on symptoms and reflux events in patients with gastro-oesophageal reflux disease. *Aliment. Pharmacol. Ther.* **2011**, *33*, 911−921.

(12) Mihov, Y.; Hasler, G. Negative Allosteric Modulators of Metabotropic Glutamate Receptors Subtype 5 in Addiction: A Therapeutic Window. *Int. J. Neuropsychopharmacol.* **2016**, *19*, pyw002.

(13) Jaeschke, G.; Kolczewski, S.; Spooren, W.; Vieira, E.; Bitter-Stoll, N.; Boissin, P.; Borroni, E.; Büttelmann, B.; Ceccarelli, S.; Clemann, N.; David, B.; Funk, C.; Guba, W.; Harrison, A.; Hartung, T.; Honer, M.; Huwyler, J.; Kuratli, M.; Niederhauser, U.; Pähler, A.; Peters, J. U.; Petersen, A.; Prinssen, E.; Ricci, A.; Rueher, D.; Rueher, M.; Schneider, M.; Spurr, P.; Stoll, T.; Tännler, D.; Wichmann, J.; Porter, R. H.; Wettstein, J. G.; Lindemann, L. Metabotropic glutamate receptor 5 negative allosteric modulators: discovery of 2-chloro-4-[1-(4-fluorophenyl)-2,5-dimethyl-1*H*-imidazol-4-ylethynyl]pyridine (basimglurant, RO4917523), a promising novel medicine for psychiatric diseases. *J. Med. Chem.* **2015**, *58*, 1358.

(14) Quiroz, J. A.; Tamburri, P.; Deptula, D.; Banken, L.; Beyer, U.; Rabbia, M.; Parkar, N.; Fontoura, P.; Santarelli, L. Efficacy and Safety of Basimglurant as Adjunctive Therapy for Major Depression: A Randomized Clinical Trial. *JAMA Psychiatry* **2016**, *73*, 675.

(15) Rutrick, D.; Stein, D. J.; Subramanian, G.; Smith, B.; Fava, M.; Hasler, G.; Cha, J. H.; Gasparini, F.; Donchev, T.; Ocwieja, M.; Johns, D.; Gomez-Mancilla, B. Mavoglurant Augmentation in OCD Patients Resistant to Selective Serotonin Reuptake Inhibitors: A Proof-of-Concept, Randomized, Placebo-Controlled, Phase 2 Study. *Adv. Ther.* **2017**, *34*, 524.

(16) Ribeiro, F. M.; Vieira, L. B.; Pires, R. G.; Olmo, R. P.; Ferguson, S. S. Metabotropic glutamate receptors and neurodegenerative diseases. *Pharmacol. Res.* **2017**, *115*, 179−191.

(17) Hoffmann, J.; Charles, A. Glutamate and Its Receptors as Therapeutic Targets for Migraine. *Neurotherapeutics* **2018**, *15*, 361.

(18) Mazzitelli, M.; Presto, P.; Antenucci, N.; Meltan, S.; Neugebauer, V. Recent Advances in the Modulation of Pain by the Metabotropic Glutamate Receptors. *Cells.* **2022**, *11*, 2608.

(19) Zhang, L.; Balan, G.; Barreiro, G.; Boscoe, B. P.; Chenard, L. K.; Cianfrogna, J.; Claffey, M. M.; Chen, L.; Coffman, K. J.; Drozda, S. E.; Dunetz, J. R.; Fonseca, K. R.; Galatsis, P.; Grimwood, S.; Lazzaro, J. T.; Mancuso, J. Y.; Miller, E. L.; Reese, M. R.; Rogers, B. N.; Sakurada, I.; Skaddan, M.; Smith, D. L.; Stepan, A. F.; Trapa, P.; Tuttle, J. B.; Verhoest, P. R.; Walker, D. P.; Wright, A. S.; Zaleska, M. M.; Zasadny, K.; Shaffer, C. L. Discovery and Preclinical Characterization of 1-Methyl-3-(4-methylpyridin-3-yl)-6-(pyridin-2-ylmethoxy)-1*H*-pyrazolo-[3,4-*b*]pyrazine (PF470): A Highly Potent, Selective, and Efficacious Metabotropic Glutamate Receptor 5 ($mGluR_5$) Negative Allosteric Modulator. *J. Med. Chem.* **2014**, *57*, 861.

(20) Varnäs, K.; Cselényi, Z.; Arakawa, R.; Nag, S.; Stepanov, V.; Moein, M. M.; Johnström, P.; Kingston, L.; Elmore, C. S.; Halldin, C.; Farde, L. The pro-psychotic metabotropic glutamate receptor compounds fenobam and AZD9272 share binding sites with monoamine oxidase-B inhibitors in humans. *Neuropharmacology* **2020**, *162*, 107809.

(21) Bennett, K. A.; Christopher, J. A.; Tehan, B. G. Structure-based discovery and development of metabotropic glutamate receptor 5 negative allosteric modulators. *Adv. Pharmacol.* **2020**, *88*, 35.

(22) Felts, A. S.; Rodriguez, A. L.; Blobaum, A. L.; Morrison, R. D.; Bates, B. S.; Thompson Gray, A.; Rook, J. M.; Tantawy, M. N.; Byers, F. W.; Chang, S.; Venable, D. F.; Luscombe, V. B.; Tamagnan, G. D.; Niswender, C. M.; Daniels, J. S.; Jones, C. K.; Conn, P. J.; Lindsley, C. W.; Emmitte, K. A. Discovery of *N*-(5-Fluoropyridin-2-yl)-6-methyl-4-(pyrimidin-5-yloxy)picolinamide (VU0424238): A Novel Negative Allosteric Modulator of Metabotropic Glutamate Receptor Subtype 5 Selected for Clinical Evaluation. *J. Med. Chem.* **2017**, *60*, 5072.

(23) Crouch, R. D.; Blobaum, A. L.; Felts, A. S.; Conn, P. J.; Lindsley, C. W. Species-Specific Involvement of Aldehyde Oxidase and Xanthine Oxidase in the Metabolism of the Pyrimidine-Containing $mGlu_5$-Negative Allosteric Modulator VU0424238 (Auglurant). *Drug Metab. Dispos.* **2017**, *45*, 1245−1259.

(24) Felts, A. S.; Bollinger, K. A.; Brassard, C. J.; Rodriguez, A. L.; Morrison, R. D.; Daniels, J. S.; Blobaum, A. L.; Niswender, C. M.; Jones, C. K.; Conn, P. J.; Emmitte, K. A.; Lindsley, C. W. Discovery of 4-alkoxy-6-methylpicolinamide negative allosteric modulators of metabotropic glutamate receptor subtype 5. *Bioorg. Med. Chem. Lett.* **2019**, *29*, 47−50.

(25) Barbaro, L.; Rodriguez, A. L.; Blevins, A. N.; Dickerson, J. W.; Billard, N.; Boutaud, O.; Rook, J. L.; Niswender, C. M.; Conn, P. J.; Engers, D. W.; Lindsley, C. W. Discovery of "Molecular Switches" within a Series of $mGlu_5$ Allosteric Ligands Driven by a "Magic Methyl" Effect Affording Both PAMs and NAMs with In Vivo Activity, Derived from an M1 PAM Chemotype. *ACS Bio. Med. Chem. Au.* **2021**, *1*, 21−30.

https://doi.org/10.1021/acsmedchemlett.5c00119
ACS Med. Chem. Lett. 2025, 16, 865−874